

GRB 090323 and GRB 090328: two long high-energy GRBs detected with Fermi

E. BISSALDI

ON BEHALF OF THE FERMI/GBM TEAM

Max-Planck-Institut für extraterrestrische Physik,
Giessenbachstrasse 1, 85748 Garching, Germany

Abstract

We present the analysis of two long Gamma-Ray Bursts, GRB 090323 and GRB 090328, which triggered the Fermi Gamma-Ray Burst Monitor (GBM) and generated an Autonomous Repoint Request to the Fermi Large Area Telescope. The GBM light curves show multi-peaked structures for both events. Here, we present time-integrated and time-resolved burst spectra fitted with different models by the GBM detectors.

1 Introduction

The Fermi Gamma-ray Space Telescope is an international and multi-agency space observatory, whose payload comprises two science instruments, the Large Area Telescope (LAT, 20 MeV–300 GeV) [1] and the GBM [2]. The primary role of GBM is to augment the science return from Fermi in the study of Gamma-Ray Bursts (GRBs) by discovering transient events within a larger field of view (FoV) and performing time-resolved spectroscopy of the measured burst emission. The GBM detectors comprise 12 thallium activated sodium iodide (NaI(Tl)) scintillation detectors (8–1000 keV) and two bismuth germanate (BGO) scintillation detectors (0.2–40 MeV). The individual NaI detectors are mounted around the spacecraft and their axes are

oriented such that the positions of GRBs can be derived from the measured relative counting rates. The two BGO detectors are mounted on opposite sides of the Fermi spacecraft, covering a net ~ 8 sr FoV, and provide the overlap in energy with the LAT instrument.

2 Observations of GRB 090323 and GRB 090328

As of December 11, 2009, the LAT detected 14 GRBs at energies above 100 MeV. In the following sections, we report the observations and analysis of gamma-ray emission from two GRBs detected within a week of each other in late March 2009, namely GRB 090323 and GRB 090328. These bursts have several interesting features. They were bright enough to trigger an autonomous repointing of the spacecraft, thus allowing observations by the LAT for five hours (subject to Earth avoidance). Moreover, the bursts were detected by the LAT Automated Science Processing (ASP) by using 6 hours of data. The improved locations obtained by the LAT instruments made it possible to follow-up the bursts in the X-ray and in the optical, thus providing spectroscopic redshifts of $z = 3.6$ [3], and $z = 0.736$ [4], respectively. Moreover, there is evidence of emission detected in the LAT up to late times, which will be extensively discussed in [5]. Here, we will mainly focus on the GBM analysis of these events, including temporal and spectral properties, both time-integrated and time-resolved.

3 GBM light curves

On 2009 March 23 at 00:02:42.63 UT, the GBM triggered on and localized GRB 090323 (trigger 259459364/090323002). Significant emission was observed in all NaI detectors on the same spacecraft side (NaI 6 to NaI 11) up to 500 keV. Moreover, BGO detector 1 detected the burst up to about 3 MeV. Due to the repointing maneuver, the detectors' angles with respect to the burst location had to be carefully examined over the whole burst duration. For some detectors, the angle changed over about 13° . This is a crucial step before computing the correct detector response matrices (DRMs) for each individual detector over a particular burst interval. The GRB light curve is shown in Figure 1 (*left panel*) and is characterized by a first group of peaks showing a lot of substructure between the trigger time (T_0) and T_0+70 s, a plateau with very little emission from T_0+70 s to $\sim T_0+110$ s and finally three late well-defined and equally-spaced peaks, each about 10 s long. By combining the orientation changes with the peculiarities of

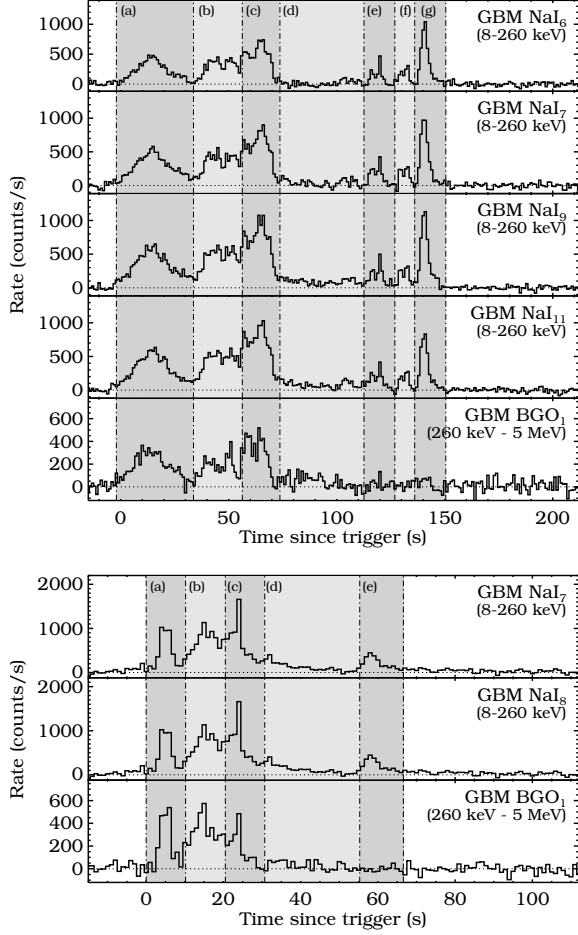


Figure 1 Light curves of GRB 090323 (*top*) and GRB 090328 (*bottom*) observed by the GBM detectors, from lowest to highest energies. The *top four (two) panels* show the background-subtracted count rates, in the 8–260 keV energy band, of the four (two) most illuminated NaI detectors. For both bursts, the *bottom panel* is the corresponding plot for BGO detector 1, between 260 keV and 5 MeV. The vertical dash-dotted lines indicate the time intervals used in the time-resolved spectral analysis. In all cases, the bin width is 1 s.

the GRB profile, the burst was divided in seven intervals (**a** to **g**) for the spectral analysis. The burst characteristic durations T_{90} and T_{50} , which represent the time during which 90% and 50% of the event flux is collected

[6], were found to be 133.1 ± 1.4 s and 42 ± 4 s, respectively, where the error bars reflect the 1-sigma statistical uncertainties.

On 2009 March 28 at 09:36:46.51 UT, the GBM triggered on and localized GRB 090328 (trigger 259925808/090328401). Significant emission was observed in nine NaI detectors, including all detectors on one side of the spacecraft (NaI 6 to NaI 11) plus NaI 3 and NaI 4. The burst was detected by BGO detector 1 up to about 2 MeV. NaI 7 and NaI 8 are relatively stable in orientation during the spacecraft slew (the angles change over $\sim 4^\circ$ only) and represent the best choice for the spectral analysis. Light curves for GRB 090328 are shown in the *right panel* of Figure 1. The burst profile is similar to the one of GRB 090323, displaying three emission peaks followed by a decreasing plateau phase and final peak which is mainly detected in the NaI detectors. However, GRB 090328 has a much shorter duration with $T_{90} = 57 \pm 3$ s and $T_{50} = 15.4 \pm 1.0$ s. For the spectral analysis, the burst was divided in five intervals (**a** to **e**).

4 Time-resolved spectral analysis

Spectral analysis was performed for both GRBs using the GBM data only. The NaI data are usually fit from 8 keV to 1 MeV and the BGO data from 250 keV to 40 MeV using the TTE data type [2]. The fits were performed with the spectral analysis software package RMFIT (version 3.2). For the spectral analysis, the best NaI detector pair was fitted together with detector BGO 1 with various spectral models, i.e. (i) a simple power-law (PL) function; (ii) a power-law function with an exponential high-energy cutoff (Comptonized), where the cutoff energy is parameterized as E_{peak} ; and (iii) a typical GRB Band function [7]. The time-integrated spectrum of GRB 090323 is best modeled by a Band function with an E_{peak} of about 600 keV. In the case of GRB 090328, the time-integrated spectrum is best modeled by a power-law with exponential high-energy cutoff with an E_{peak} of about 750 keV.

Results for the time-resolved spectral analysis of GRB 090323 and GRB 090328 are given in Table 1. Spectral evolution throughout both GRBs is apparent from the changing E_{peak} values. The highest E_{peak} is measured during the first emission episode (interval **a**) for GRB 090323 and during the second emission episode (interval **b**) for GRB 090328. Both intervals are best fitted by a Band model. The counts spectra are also shown in Figure 2.

Table 1. Fit parameters for the time-resolved spectral fits of GRB 090323 and GRB 090328.

Interval	Det.	Time range (s)	Model	$E_{\text{peak}}^{\text{a}}$ (keV)	α^{b}	β^{c}	γ^{d}	CSTAT/ DOF	Energy fluence (erg cm $^{-2}$, 8 keV–1 MeV)
GRB 090323									
...	n9,b1	-2.0–150.5	<i>Band</i>	591 ($^{+36}_{-33}$)	-1.05 (± 0.02)	-2.7 ($^{+0.2}_{-0.4}$)	...	888/237	$(1.22 \pm 0.02) \times 10^{-4}$
a.	n9,nb,b1	-2.0–33.8	<i>Band</i>	710 ($^{+78}_{-67}$)	-0.94 (± 0.03)	-2.3 ($^{+0.1}_{-0.2}$)	...	474/356	$(3.48 \pm 0.06) \times 10^{-5}$
b.	n9,nb,b1	33.8–56.3	<i>Comp</i>	447 ($^{+25}_{-23}$)	-0.81 (± 0.03)	517/357	$(2.72 \pm 0.04) \times 10^{-5}$
c.	n9,nb,b1	56.3–73.7	<i>Comp</i>	521 ($^{+23}_{-22}$)	-0.84 (± 0.02)	475/357	$(3.47 \pm 0.04) \times 10^{-5}$
d.	n9,nb,b1	73.7–112.6	<i>PL</i>	-1.57 (± 0.02)	663/359	$(1.06 \pm 0.02) \times 10^{-5}$
e.	n7,n9,b1	112.6–127.0	<i>Comp</i>	200 ($^{+40}_{-30}$)	-1.18 (± 0.09)	437/358	$(3.76 \pm 0.22) \times 10^{-6}$
f.	n7,n9,b1	127.0–136.2	<i>Comp</i>	154 ($^{+34}_{-22}$)	-1.07 ($^{+0.14}_{-0.13}$)	371/358	$(2.34 \pm 0.14) \times 10^{-7}$
g.	n6,n9,b1	136.2–150.5	<i>Band</i>	108 ($^{+13}_{-14}$)	-1.00 ($^{+0.11}_{-0.09}$)	-2.3 (± 0.2)	...	450/358	$(5.99 \pm 0.22) \times 10^{-6}$
GRB 090328									
...	n7,n8,b1	0.0–66.6	<i>Comp</i>	744 ($^{+50}_{-47}$)	-1.07 (± 0.02)	644/360	$(5.09 \pm 0.04) \times 10^{-5}$
a.	n7,n8,b1	0.0–10.2	<i>Comp</i>	703 ($^{+71}_{-61}$)	-0.80 (± 0.04)	388/361	$(1.20 \pm 0.02) \times 10^{-5}$
b.	n7,n8,b1	10.2–20.5	<i>Band</i>	716 ($^{+56}_{-52}$)	-0.84 (± 0.03)	-2.4 ($^{+0.1}_{-0.2}$)	...	430/360	$(2.01 \pm 0.03) \times 10^{-5}$
c.	n7,n8,b1	20.5–30.7	<i>Band</i>	451 (± 66)	-1.07 ($^{+0.05}_{-0.04}$)	-2.2 ($^{+0.2}_{-0.3}$)	...	436/360	$(1.22 \pm 0.02) \times 10^{-5}$
d.	n7,n8,b1	30.7–55.3	<i>PL</i>	-1.52 (± 0.03)	480/362	$(4.12 \pm 0.15) \times 10^{-6}$
e.	n7,n8,b1	55.3–66.6	<i>Comp</i>	123 ($^{+33}_{-21}$)	-1.41 ($^{+0.12}_{-0.11}$)	354/361	$(1.87 \pm 0.12) \times 10^{-6}$

Note. — The time range values are relative to the trigger time T_0 .

^a Fitted E_{peak} for the Band or Comptonized models.

^b Low-energy spectral index α for the Band or Comptonized models.

^c High-energy spectral index β for the Band model.

^d Spectral index γ for the PL model.

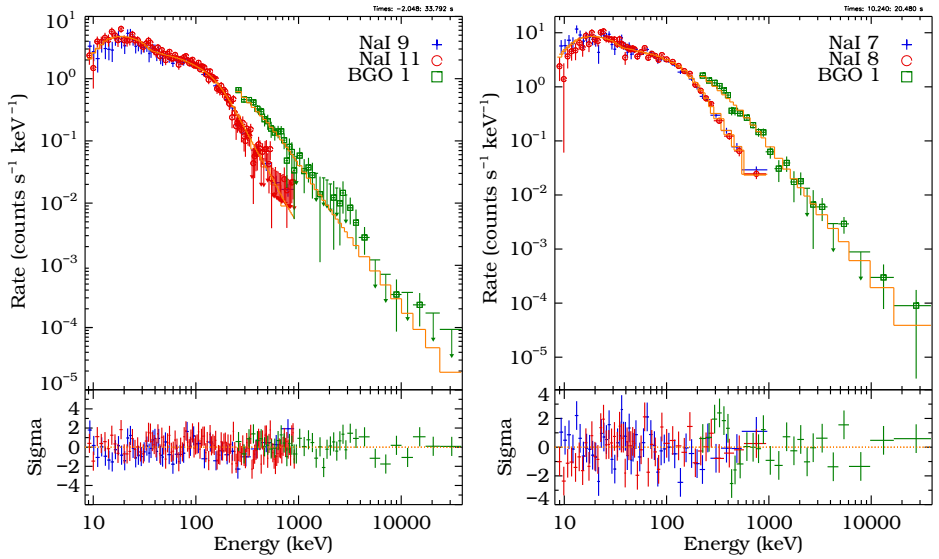


Figure 2 *Left*: Band fit of GBM data to interval **a** of GRB 090323 (from $T_0-2.0$ s to $T_0+33.7$ s); *Right*: Band fit of GBM data to interval **b** of GRB 090328 (from $T_0+10.2$ s to $T_0+20.5$ s).

References

- [1] ATWOOD W. B. ET AL., *ApJ* **697** (2009) 1071.
- [2] MEEGAN C. A. ET AL., *ApJ* **702** (2009) 791.
- [3] CHORNOCK R. ET AL., *GCN Circular* **9028** (2009).
- [4] CENKO S. B. ET AL., *GCN Circular* **9053** (2009).
- [5] ABDO A. A. ET AL., *ApJ in preparation* (2010).
- [6] KOUVELIOTOU C. ET AL., *ApJ* **413** (1993) L101.
- [7] BAND D. ET AL., *ApJ* **413** (1993) 281.